

# Estimation of Heat Evolution during Viscoelastic Crack Propagation by Liquid Crystal Film Technique

AKIRA KOBAYASHI, MASAYUKI MUNEMURA, NOBUO OHTANI, and HIROSHI SUEMASU, *Faculty of Engineering, Institute of Interdisciplinary Research, University of Tokyo, Meguro-ku, Tokyo 153, Japan*

## Synopsis

Heat generated during dynamic crack propagation in viscoelastic solids was investigated by visible liquid crystal film technique to observe the thermal boundary front emanating from a running crack tip. The crack propagation velocity was also measured by the velocity gauge method. The heat so estimated is correlated with the crack propagation velocity.

## INTRODUCTION

When a high-velocity crack runs in a viscoelastic solid, strong energy concentration is observed at the very running crack tip, as seen from previous results.<sup>1</sup> Naturally, heat evolution and subsequent heat conduction resulting in a temperature rise leading toward thermal boundary front formation are expected. Theoretically, Kambour and Barker,<sup>2</sup> Rice and Levy,<sup>3</sup> and Parvin<sup>4</sup> investigated this problem mainly on the temperature rise. However, their results showed large discrepancies in the quantitative evaluation, and further experimental verification should be required, in addition to the work by Fuller, Fox, and Field<sup>5</sup> of the Cavendish Laboratory, England, in 1975.

In the present study, the thermal boundary front emanating from the running crack tip is traced by visual liquid crystal film technique to estimate the heat evolution during dynamic crack propagation in a viscoelastic solid. The correlation between the heat evolved and the crack propagation velocity is also investigated. The crack propagation velocity is measured by the conventional velocity gauge method.

## EXPERIMENTAL

### Specimen and Experimental Procedure

A poly(methyl methacrylate) (PMMA) specimen, shown in Figure 1, is prepared from the virgin Sumipex sheet product of Sumitomo Chemical Co., Japan, and is subjected to mode I tension loading to initiate the crack propagation by an Instron-type tensile tester at room temperature. During dynamic crack propagation, the crack propagation velocity is measured by the velocity gauge method as described later, and the thermal boundary front is also photographed by the visual liquid crystal film technique (see below) leading toward the heat evolution calculation during fracture. The load is measured by a load cell.

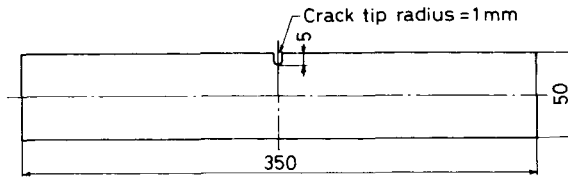


Fig. 1. Specimen dimensions.

**Velocity Gauges**

Velocity gauges consist of a series of conducting wires, du Pont No. 4817 conductive silver coating material, placed at certain intervals on the projected path of the crack propagation and perpendicular to the direction of crack propagation, as shown in Figure 2. The average crack propagation velocity between wires can be obtained from the times at which these wires break owing to the propagating crack. Further detail is given in an early report.<sup>6</sup>

**Liquid Crystal Visualization Technique**

Liquid crystal was discovered by Friedrich Reinitzer in 1888. It is of optical-anisotropy liquid generating birefringence, viz., showing mesophase. Since Ferguson of Westinghouse Research Laboratory proposed thermography by liquid crystal in 1963, this technique has often been employed as an experimental tool. More than 3000 kinds of liquid crystals now exist.

In the present investigation, cholesteric liquid crystal is employed, as this has a color sensitivity to changes in temperature and so is good for visualization of the thermal boundary front emanating from a running crack front. Actually, a mixture of 60 wt % cholesteryl oleyl carbonate and 40 wt % cholesteryl nonanoate was used. A layer about 100  $\mu\text{m}$  thick was spread over a specimen surface which was painted matt black, reverse to the velocity gauge surface. The calibration was made by using ice, water, and boiling water. The present liquid crystal film changes from red through blue as the temperature rises are shown in Figure 3. In the evolved heat calculation shown later, the thermal capacity of the film and the time taken to respond to changes in temperature were both regarded as small enough to be neglected.

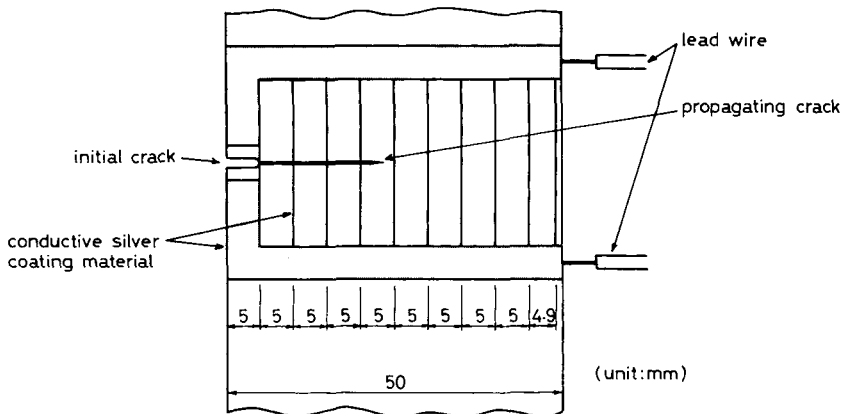


Fig. 2. Velocity gauge arrangement.

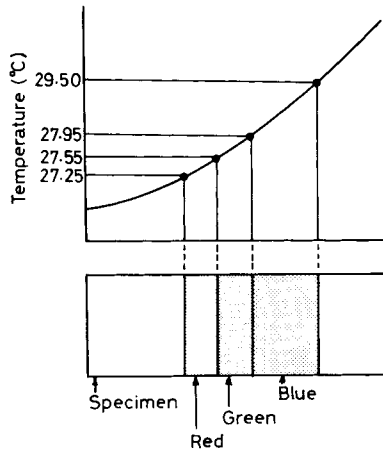


Fig. 3. Color sensitivity to changes in temperature.

**Measurement System**

Figure 4 shows the block diagram employed in the present study. The colored thermal boundary front emanating from a running crack front was photographed after fracture on Fuji ASA 400 color film by keeping the camera shutter open in the dark. The propagating crack broke the triggering conducting wires and fired an electronic flash for photographing.

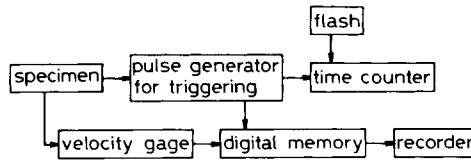


Fig. 4. Measurement system block diagram.

**HEAT EVOLUTION CALCULATION**

The heat evolved during crack propagation,  $Q$ , was calculated by the heat conduction equation combined with the thermal boundary front obtained from the color change in liquid crystal film during fracture. In performing the calculation, the following assumptions were employed:

- (1) The thermal capacity of the liquid crystal film is small enough to be neglected.
- (2) The time taken to respond to changes of temperature is small enough to be neglected.
- (3) Heat conduction is assumed to be one-dimensional heat flow.
- (4) Heat loss from the crack surface is small enough to be neglected.

Thus, the heat evolved,  $Q$ , can be expressed as<sup>7</sup>

$$Q = \rho c \sqrt{4\pi kt} T \exp\left(\frac{y^2}{4kt}\right) \tag{1}$$

In performing the calculation, the following equation was used:

$$Q = \rho c \sqrt{4\pi kt} \frac{\Delta T}{\left(-\frac{y_1^2}{4kt}\right) - \left(-\frac{y_2^2}{4kt}\right)} \tag{2}$$

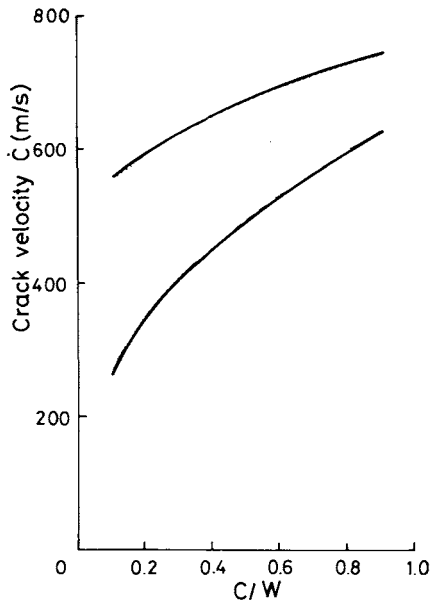


Fig. 5. Crack propagation velocity profile:  $C$  = crack length;  $W$  = specimen width.

where  $Q$  is heat evolved on both cracked surfaces per unit area of crack advance,  $k$  is thermal diffusivity =  $1.08 \times 10^{-7}$  m<sup>2</sup>/s,  $c$  is specific heat = 0.35 cal/g $\cdot$ °C,  $\rho$  is density =  $1.19 \times 10^6$  g/m<sup>3</sup>,  $t$  is time after fracture,  $\Delta T$  is temperature difference between green/blue and red/green thermal boundaries = 0.4°C,  $y_1$  is distance between green/blue thermal boundary and the cracked surface, and  $y_2$  is distance between red/green thermal boundary and the cracked surface.

## RESULTS AND DISCUSSIONS

The crack propagation velocity curves obtained are shown in Figure 5. Although there is scatter in the data, the same tendency is observed as in the previous results.<sup>6</sup> In the present result, the crack propagation is initiated by quasistatic tension loading in mode I.

Figure 6 shows an example of thermal boundary front obtained 1.44 s after fracture by the visible liquid crystal film technique. Macroscopically, the thermal boundary front forms a straight line gradually separating from the cracked surface.

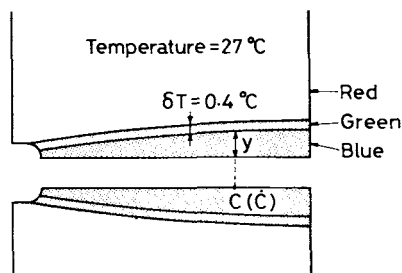


Fig. 6. Thermal boundary front obtained 1.44 s after fracture by liquid crystal film technique.

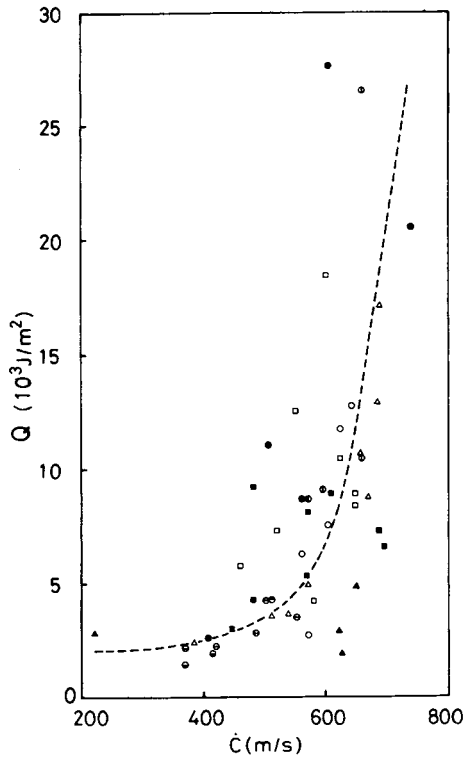


Fig. 7. Heat evolution vs. crack propagation velocity. For samples 1, 2 and 4 (○, ●, △); samples 6 through 10 (▲, □, ■, ◇, ⊖).

The evolved heat calculated by using the previous equation is shown in Figure 7 as a function of crack propagation velocity. The strong energy concentration was already observed at the running crack front in a viscoelastic solid<sup>1</sup> and also predicted theoretically by several investigators<sup>2-4</sup> as already mentioned in the

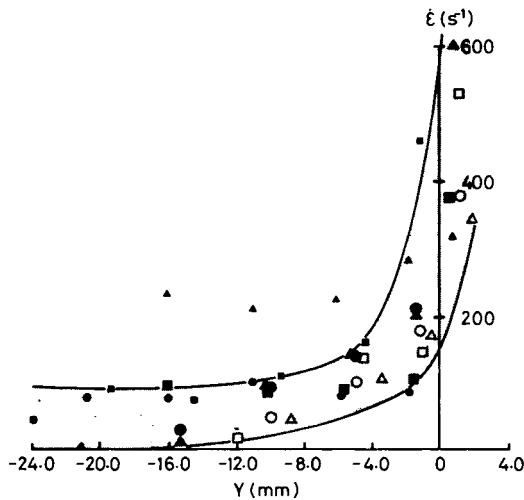


Fig. 8. Local strain rate measured as a function of distance ahead of a running crack tip.  $\dot{\epsilon}_A$  ( $s^{-1}$ )  $3.03 \times 10^{-4}$ : samples 1 through 3 (○, △, □);  $\dot{\epsilon}_A$  ( $s^{-1}$ )  $3.03 \times 10^{-2}$ : samples 5 through 10 (●, ▲, ■, ●, ▲, ■).

“Introduction.” For instance, Figure 8 shows that the local strain rate  $\dot{\epsilon}$  obtained at the running crack tip is much greater than the average strain rate  $\dot{\epsilon}_A$ , where  $\dot{\epsilon}_A$  is the crosshead speed/specimen gauge length ratio and  $Y$  is the distance from the running crack tip.<sup>1</sup>

Fuller et al.<sup>5</sup> performed the experiment on PMMA; however, their results covered a higher crack propagation velocity range of more than 400 m/s and a small-size specimen, 20 mm  $\times$  5 mm  $\times$  1.5 mm.

The obtained heat  $Q$ -vs.-crack propagation velocity  $\dot{C}$  relation in Figure 7 exhibits a result similar to that of Fuller et al., but the absolute  $Q$  value is greater in the present case. It is also apparent that  $Q$  rapidly increases when the crack propagation velocity exceeds about 600 m/s.

Mr. Hitoshi Yamada is thanked for his contribution to the present study.

### References

1. A. Kobayashi, M. Munemura, and N. Ohtani, 22nd Aircraft/Aerospace Structures and Strength Conf., Japan Soc. Aeronautical & Space Sci., 1980.
2. R. P. Kambour and R. E. Barker, *J. Polym. Sci.*, **A2**, 359 (1966).
3. J. R. Rice and N. Levy, in *Physics and Plasticity*, ed. by A. S. Argon, M.I.T. Press, Cambridge, Mass., 1969, p. 277.
4. M. Parvin, *Int. J. Fracture*, **15** (5), 397 (1979).
5. K. N. G. Fuller, P. G. Fox, and J. E. Field, *Proc. Roy. Soc. London*, **A341**, 537 (1975).
6. A. Kobayashi, N. Ohtani, and T. Sato, *J. Appl. Polym. Sci.*, **18**, 1625 (1974).
7. H. S. Carslaw and J. C. Jaeger, *Conduction of Heat in Solids*, Oxford University Press, New York, 1959.

Received November 25, 1981

Accepted March 29, 1982